Journal of Physics B: Atomic,
Molecular and Optical Physics

PAPER

Effective collision cross section of xenon plasma debris in argon buffer gas

To cite this article: Tomoaki Inoue *et al* 2012 *J. Phys. B: At. Mol. Opt. Phys.* **45** 115401

J. Phys. B: At. Mol. Opt. Phys. **45** (2012) 115401 (5pp) doi:10.1088/0953-4075/45/11/115401

Effective collision cross section of xenon plasma debris in argon buffer gas

Tomoaki Inoue, Takayasu Mochizuki, Kazuya Masuda, Sho Amano, Tsuguhisa Sekioka and Kazuhiro Kanda

Laboratory of Advanced Science and Technology for Industry, University of Hyogo 3-1-2 Kouto, Kamigori, Ako-gun, Hyogo 678-1205, Japan

E-mail: t-inoue@lasti.u-hyogo.ac.jp

Received 11 January 2012, in final form 12 April 2012
Published 18 May 2012
Online at stacks.iop.org/JPhysB/45/115401

Abstract
Mitigation of fast debris and soft x-rays generated from laser-produced xenon plasmas were studied in an argon buffer gas in laser intensities of 10^9–10^{11} W cm^{-2} using a cryogenic drum target. Considerable mitigation of debris was confirmed by measurements of material sputtering. From the experimental results, an attenuation parameter of sputtering by the debris $\bar{\sigma}_1$ and an absorption cross section of soft x-rays at 13.5 nm σ_2(13.5 nm) were derived to be 2.2×10^{-20} m^2 and 1.8×10^{-22} m^2, respectively. Moreover, $\bar{\sigma}_1$ is concluded to be equivalent to the effective collision cross section σ_1 of a debris particle at kinetic energy of 1–4 keV. Sufficient debris mitigation can be obtained together with low soft x-ray absorption (less than 10%). These parameters provide a useful design tool for realizing a practical soft x-ray source because they predict the effect of the buffer gas well.

(Some figures may appear in colour only in the online journal)

1. Introduction

Soft x-rays from high-temperature, high-density plasmas produced by focusing a high-intensity laser on target materials are expected to be useful as a compact high-brightness soft x-ray source for a variety of applications [1–3]. However, debris emitted from the plasmas remains one of the most serious problems that must be solved before the source can be used for practical applications. The debris generally causes sputtering and/or deposition on the surfaces of condenser mirrors [4], degrading the mirrors' reflectivity and thus reducing the usable x-ray output power. Bollanti's group [5] demonstrated a simple but efficient mitigation method [6] in which plasma debris from metallic targets such as tantalum and copper was mitigated by a buffer gas [7–9].

Chemically inert xenon debris from a xenon plasma target will not be deposited on the mirror surface [4]. Thus, mitigation of fast xenon debris by the buffer gas is a technical issue to be resolved. However, a trade-off between mitigation of the fast debris and absorption of the soft x-rays, both of which are caused by the buffer gas, remains to be studied. On the other hand, the debris mitigation process consists, in principle, of various types of collisions with the buffer gas molecules, which contain ions in various charge states with wide kinetic energy distributions. Therefore, an effective attenuation parameter as a function of the buffer gas density is required as a design tool for realizing a practical soft x-ray source. Unfortunately, no effective attenuation figure that can be of practical use for scaling the debris mitigation by the buffer gas has been reported, to the best of our knowledge.

The use of an argon gas buffer seems to be most practical because transmission of soft x-rays in argon gas is much higher than that in xenon gas, although it is slightly lower than that in krypton gas. In addition, argon gas costs much less than either krypton or xenon gas.

In this paper, we report the experimental results and discuss the effective attenuation cross sections of plasma debris and soft x-rays in argon buffer gas. We find an effective debris mitigation parameter that is useful for realizing a practical laser-produced soft x-ray source.

2. Experimental details

A rotating drum cryogenic solid xenon target was used. Details of the drum target are available elsewhere [10]; we describe it briefly here. A solid xenon layer was formed by spraying xenon gas on the surface of the drum which was kept at a temperature of approximately 192 K. The drum was rotated at 130 rpm so that a fresh xenon surface could be supplied with each laser shot. The thickness of the xenon layer was adjusted to about 500 μm by two wipers installed inside the drum's cover. A Q-switched 1.06 μm Nd:yttrium aluminium garnet laser (Quantel YG980) pulse was focused through a f/500 lens on the target surface at an angle of 5° to normal incidence. The laser pulse duration was 8 ns at full-width at half-maximum with an energy of 300 mJ/pulse for either single shot or repetitive shots at 10 Hz. The laser intensity was adjusted in a range of 10^9–10^{11} W cm^{-2} by changing the lens position. The target chamber was evacuated by a turbo-molecular pump that maintained a xenon pressure in the chamber of less than 0.2 Pa except when the argon buffer gas was present. The argon gas at room temperature was introduced into the chamber through a nozzle on an upper wall of the chamber.

Soft x-ray emission spectra in a wide wavelength range of 5–17 nm [11] were observed by a transmission grating spectrometer [12, 13] in order to obtain the x-ray conversion efficiency (CE). Although soft x-rays in this wide wavelength range are useful for a variety of applications, we measured as a reference only the energy transmission of soft x-rays at 13.5 nm [3] through the buffer gas as a function of the gas density. A soft x-ray calorimeter consisting of an x-ray photodiode and a Mo/Si mirror was mounted at a distance of 190 mm and −22.5° from the plasma source to measure the soft x-ray pulse energy at 13.5 nm. Faraday cups (FC) were mounted at 45° and 22.5° to measure the current signals and velocities of the ion debris. It was difficult to obtain a reliable FC ion signal with argon gas because strong photo-ionizations took place causing strong photo-current which continued to flow in a long time period. Therefore, we measured the FC current only without gas. A Thomson parabola spectrometer [14] was also mounted at 45° to identify the charge numbers of the ion debris.

The fast debris included ions as well as neutral particles. Therefore, we measured the mitigation of the fast debris indirectly by monitoring the sputtering effect they caused. The obtained mitigation rate of the sputtering provides practical information for evaluating the damage to the mirror. To evaluate the sputtering rate, we used a gold-coated quartz crystal microbalance (QCM: INFICON, SQM-160) mounted at a distance of 77 mm and an angle of 45°. The QCM measured the deposited or sputtered mass per unit area on the QCM by monitoring a shift in the resonance frequency of the gold-coated quartz vibrator. An advantage of the QCM is that it provides the total absolute sputtering rate due to bombardment by both fast ion debris and fast neutral particles. We stacked many laser shots from the Quantel laser because the QCM had relatively poor sensitivity. A micro-channel plate (MCP) detector was mounted at 45° to observe ion and fast neutral debris separately in combination with a pair of electrostatic deflecting electrodes mounted in front of the MCP.

The sputtering rate and the absorption rate at 13.5 nm were measured using the QCM and soft x-ray calorimeter, respectively, as a function of the argon gas pressure, which was varied by adjusting the flow rate of the argon gas.

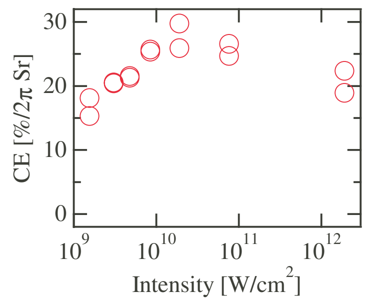

Figure 1. Laser intensity dependence of CE of soft x-rays (5–17 nm) at a laser wavelength of 1 μm.

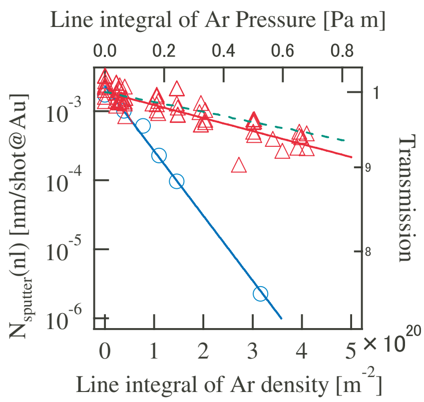

Figure 2. Mitigation of Au sputtering by fast xenon debris (○) and transmission of 13.5 nm soft x-rays (Δ; experimental, dotted line; Henke *et al* [19]) as a function of the line integral of the argon pressure and the argon gas density from the source to the observation point.

3. Results and discussion

X-ray emission experiments were performed with the rotating drum cryogenic xenon target. We obtained the laser intensity dependence of the soft x-ray CEs at 5–17 nm, as shown in figure 1. The laser intensity range at which the CE is significant is found to be 10^9–10^{11} W cm^{-2}.

The circles and triangles in figure 2 represent the sputtering rate $N_{\text{sputter}}(nl)$ and transmission of soft x-rays $T(nl)$ at 13.5 nm, respectively, which were experimentally obtained as a function of the line integral of the argon pressure and the argon gas density from the source to the observation point. Here, nl should be expressed more precisely by $\int n\mathrm{d}l$, but we assumed that n was uniform in a spatial range of interest for observing the buffering effect. Figure 2 confirms that considerable mitigation of the debris occurred. The amount of fast debris arriving at the observation position after collision with gas molecules is expressed by

$$\frac{N_{\text{Xe}}(nl, E, Z)}{N_{\text{Xe}}(0, E, Z)} = \exp(-\sigma_1(E, Z)nl), \quad (1)$$

where $N_{\text{Xe}}(nl, E, Z)$ and $N_{\text{Xe}}(0, E, Z)$ are the number of debris particles per unit energy interval arriving at the observation point which is located at a distance l from the source with and without a buffer gas of density n, respectively. $\sigma_1(E, Z)$ is the collision cross section of a debris particle colliding with gas molecules. These parameters generally depend on the kinetic energy E and charge number Z of the fast debris. From the behaviour of the exponential attenuation of the sputtering in figure 2, we assume that the number of debris particles reaching the observation point is reduced in collisions with gas molecules.

Note that the experimentally observed $N_{\text{sputter}}(nl)$ decreased in an approximately exponential form as nl increased, as shown in figure 2. Thus, we assume that $N_{\text{sputter}}(nl)$ is well described by

$$N_{\text{sputter}}(nl) = N_{\text{sputter}}(0)\exp(-\bar{\sigma}_1 nl), \tag{2}$$

where $\bar{\sigma}_1$ is the attenuation parameter of sputtering for the argon gas buffer. It has the same unit as a cross section. Similarly, $T(nl)$ is expressed by

$$T(nl) = \exp(-\sigma_2(13.5\text{ nm})nl), \tag{3}$$

where $\sigma_2(13.5\text{ nm})$ is the absorption cross section of soft x-rays at 13.5 nm for an argon molecule. From figure 2, $\bar{\sigma}_1$ and $\sigma_2(13.5\text{ nm})$ were derived to be $2.2 \times 10^{-20}\text{ m}^2$ and $1.8 \times 10^{-22}\text{ m}^2$, respectively.

Using the number of debris particles per unit energy interval $N_{\text{Xe}}(nl, E, Z)$, we express $N_{\text{sputter}}(nl)$ as

$$N_{\text{sputter}}(nl) = \sum_{Z=0}^{\infty}\int s(m, E)N_{\text{Xe}}(nl, E, Z)\,\mathrm{d}E, \tag{4}$$

where $s(m, E)$ is the average number of particles sputtered by a debris particle having a mass m and kinetic energy E. Note that $s(m, E)$ depends on the mass m and kinetic energy E of the colliding debris, and also on the bombarded target material, but not on the charge number Z. We assume the effective charge number in the target material [15] as discussed later. By differentiating (2) with respect to n and substituting (1), (2) and (4) therein, we obtain

$$\bar{\sigma}_1 = \frac{-1}{l}\frac{\frac{\mathrm{d}}{\mathrm{d}n}\sum_{Z=0}^{\infty}\int s(m, E)N_{\text{Xe}}(0, E, Z)\exp(-\sigma_1(E, Z)nl)\,\mathrm{d}E}{\sum_{Z=0}^{\infty}\int s(m, E)N_{\text{Xe}}(nl, E, Z)\,\mathrm{d}E}.$$

After modifying the above equation, we obtain

$$\bar{\sigma}_1 = \frac{\sum_{Z=0}^{\infty}\int \sigma_1(E, Z)s(m, E)N_{\text{Xe}}(nl, E, Z)\,\mathrm{d}E}{\sum_{Z=0}^{\infty}\int s(m, E)N_{\text{Xe}}(nl, E, Z)\,\mathrm{d}E}. \tag{5}$$

By a similar formulation, the absorption cross section for soft x-rays $\bar{\sigma}_2$ is expressed by

$$\bar{\sigma}_2 = \frac{\int E(\lambda)\sigma_2(\lambda)\,\mathrm{d}\lambda}{\int E(\lambda)\,\mathrm{d}\lambda}, \tag{6}$$

where $E(\lambda)$ and $\sigma_2(\lambda)$ are the spectral intensities of soft x-rays at a wavelength λ and the soft x-ray absorption cross section at λ, respectively.

Using the Thomson parabola spectrometer, we determined the average charge number of ions $\bar{Z}$ to be 2 in the rotating drum target at a laser intensity of about 10^{10} W cm^{-2} [14]. It would be explained physically by a possible increase in the surface temperature of the target layer caused by the two wipers in the rotating drum, which would form a dense xenon gas layer on the surface of the cryogenic target [11]. Such a gas layer would work as a thin buffer gas layer that not only mitigates but also recombines the fast ion debris emitted from an inner high-density plasma region with cold electrons. That is, the debris generated in the hot, dense plasma was injected into the argon buffer gas after passing through the thin xenon gas layer. The above explanation is supported by the fact that the FC signal decreased by a factor of approximately 10 compared with when the drum was stationary [16]. This suggests that debris ejected from the target surface consists mainly of ions, although a small fraction of approximately 10% or less of the ion debris may have been charge-exchanged to neutral debris within the thin xenon gas layer. The signals from the MCP indicated that the ratio of fast ions to fast neutral debris particles was 10:1 [16], assuming that the MCP gain was the same for both [17]. Therefore, the major process in the argon buffer gas is concluded to be single collision between gas molecules and plasma-ion debris.

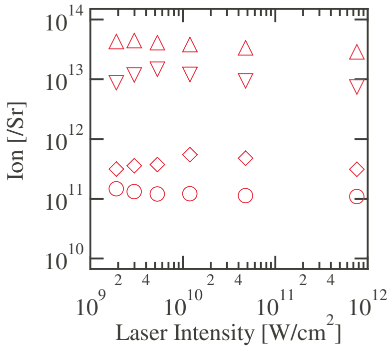

Figure 3. Laser intensity dependence of ion energy distributions for 0.3–1 keV (△), 1–4 keV (▽), 4–7 keV (◇) and 7–10 keV (○).

By using the time-of-flight signals from the FC, we obtained the laser intensity dependence of the kinetic energy distribution of ion debris without the buffer gas, as shown in figure 3. The energy distribution of the ion debris does not vary significantly, and the kinetic energies of more than 95% of the ion debris are less than 4 keV at the laser intensities of 10^9–10^{11} W cm^{-2}.

To evaluate $\bar{\sigma}_1$ using (5), the kinetic energy dependence of $s(m, E)$ was calculated by the numerical code The Stopping Range of Ions in Matter (SRIM) [18], as shown in figure 4. The $s(m, E)$ values of mirror materials such as Au, Mo, Si and Be were calculated at normal incidence, and that of Ru was calculated at an incidence angle of 70°, which is the critical angle of Ru at a wavelength of 11 nm. The values of $s(m, E)$ for the above sputtered materials were normalized by those at a kinetic energy of 4 keV.

Figure 4 shows that $s(m, E)\cdot N_{\text{Xe}}(0, E, \bar{Z})$ has significant values only at energies of 1–4 keV. Thus, we can take a representative average value $\overline{s(m, E)\cdot N_{\text{Xe}}(nl, E, Z)}$ as $s(m, E)\cdot N_{\text{Xe}}(nl, E, \bar{Z})$ in (5) for each mirror material in this energy range. The value of $\sigma_1(E, \bar{Z})$ averaged over 1–4 keV should be equivalent to $\bar{\sigma}_1$:

$$\bar{\sigma}_1 \approx \sigma_1. \tag{7}$$

Hereafter, we define $\bar{\sigma}_1$ as the effective collision cross section of a debris particle colliding with a buffer argon gas molecule. Figure 5 shows the mitigations of sputtering and ions as a function of argon gas pressure. The ion flux reaching the FC was evaluated by combining the FC signal with xenon stopping ranges obtained by the SRIM code. The normalized number

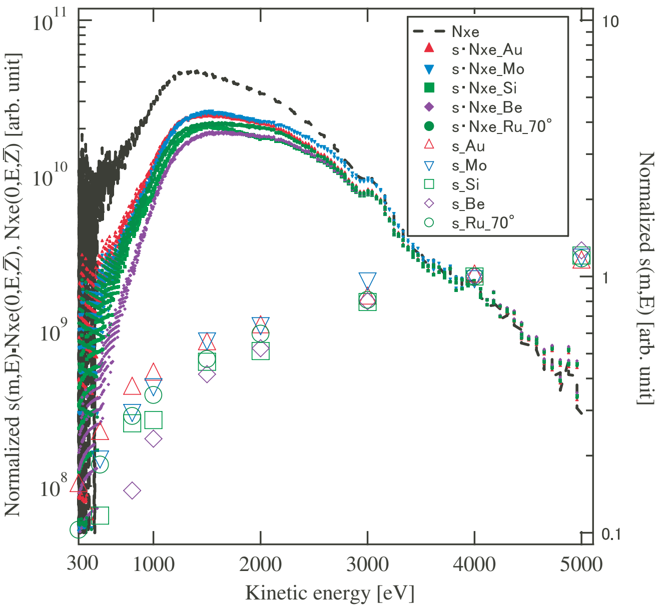

Figure 4. Kinetic energy dependences of the number of xenon ions $N_{\mathrm{Xe}}(0, E, \bar{Z})$ (dot line) and the sputtering rates $s(m, E)$ calculated by SRIM (Δ Au, ∇; Mo, □; Si, ◊ Be, ○; Ru_70°) and $s(m, E) \cdot N_{\mathrm{Xe}}(0, E, \bar{Z})$ (▲; Au, ▼; Mo, ■; Si, ■; Be, •; Ru_70°). The $s(m, E)$ values are normalized by the value at a kinetic energy of 4 keV.

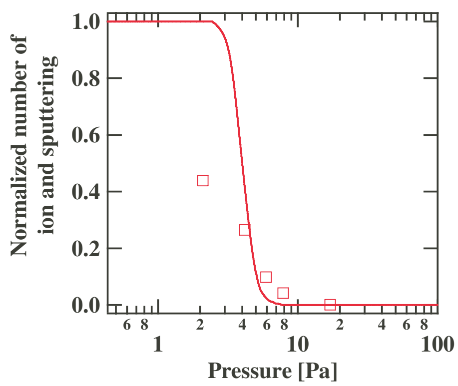

Figure 5. Argon pressure dependence of the ion flux calculated by using stopping ranges obtained by the SRIM code and FC signal (solid line), to compare with experimental results of the QCM sputtering (□).

of the sputtering was obtained experimentally as indicated by a square box. Figure 5 indicates that most of the ions are well mitigated in a range from 2 to 5 Pa. The mitigation rate of the sputtering over 4 Pa is in good agreement with that of the ion flux evaluated by using SRIM.

$\bar{\sigma}_2$ is found to be equal to the average value of the absorption cross section $\sigma_2(\lambda)$ multiplied by the spectral intensities of soft x-rays $E(\lambda)$ as a weight function. Hereafter, we define it as the effective absorption cross section. The obtained σ_2(13.5 nm) value agrees well with that in the report by Henke *et al* [19], which is about 1.4×10^{-22} m^2 at 13.5 nm. The value of $\bar{\sigma}_2$ can be derived using (6) by substituting the experimentally obtained spectral intensity of soft x-rays $E(\lambda)$ and the absorption cross section $\sigma_2(\lambda)$ from [19]. Therefore, sufficient debris mitigation can be obtained together with low soft x-ray absorption (less than 10%).

4. Conclusion

To realize a laser-produced xenon plasma soft x-ray source for applications, mitigation of fast debris and soft x-rays at 13.5 nm generated from a laser-produced xenon plasma were studied in an argon buffer gas at laser intensities of 10^9–10^{11} W cm^{-2} using a rotating drum cryogenic xenon target. The attenuation rates of debris sputtering and soft x-rays at 13.5 nm were measured as a function of the argon gas density. Considerable debris mitigation was confirmed by measurements of material sputtering. The attenuation parameter of sputtering by the debris $\bar{\sigma}_1$ is concluded to be equivalent to the effective collision cross section σ_1 of a debris particle at kinetic energies of 1–4 keV. From figure 2, $\bar{\sigma}_1$ and σ_2(13.5 nm) were evaluated as 2.2×10^{-20} m^2 and 1.8×10^{-22} m^2, respectively. Therefore, sufficient debris mitigation and low absorption of soft x-rays (less than 10%) can be obtained. The obtained parameters are useful as a design tool for realizing a practical laser-produced plasma soft x-ray source because they predict the effects of a buffer gas well.

Acknowledgment

Part of this work was supported by a grant-in-aid for Scientific Research C (21560752) from The Ministry of Education, Culture, Sports, Science and Technology of Japan (MEXT).

References

[1] Kondo H, Tomie T and Shimizu H 1996 *Appl. Phys. Lett.* **69** 182
[2] Matsuo N, Uejukkoku K, Heya A, Amano S, Takanashi Y, Miyamoto S and Mochizuki T 2007 *Japan. J. Appl. Phys.* **46** 1061
[3] Bakshi V 2005 *EUV Source for Lithography* (Bellingham, WA: SPIE Optical Engineering Press) p 4
[4] Mochizuki T 2000 *Proc. SPIE* **3886** 306
[5] Baldacchini G, Bollanti S, Onti A, Di Lazzaro P, Flora F, Mezi L, Murra D, Torre A and Zhang C Mitigation of debris emitted by plasma sources: theoretical and experimental results at ENEA http://www.sematech.org/meetings/archives/litho/7470/Poster/FinalS1/1-SO-22%20Flora_ENEA%20Poster.pdf
[6] Flora F, Mezi L, Bollanti S, Bonfigli F, Di Lazzaro P, Letardi T and Zheng C 2001 *Proc. SPIE* **4504** 77
[7] Bakshi V 2005 *EUV Source for Lithography* (Bellingham, WA: SPIE Optical Engineering Press) pp 998–1000
[8] Harilal S S, O'Shay B, Tao Y and Tillack M S 2007 *Appl. Phys.* B **86** 547
[9] Harilal S S 2007 *J. Appl. Phys.* **102** 123306
[10] Fukugaki K, Amano S, Shimoura A, Inoue T, Miyamoto S and Mochizuki T 2006 *Rev. Sci. Instrum.* **77** 063114
[11] Inoue T, Mochizuki T, Miyamoto S, Amano S, Watanabe T and Kanda K 2001 *Japan. J. Appl.* **50** 098001
[12] Eidmann K, Kuhne M, Muller P and Tsakiris G D 1990 *J. X-Ray Sci. Technol.* **2** 259
[13] Li Y, Tsakiris G D and Sigel R 1995 *Rev. Sci. Instrum.* **66** 80
[14] Sekioka T, Amano S, Inoue T and Mochizuki T 2009 *LASTI Annu. Rep.* **11** 22

[15] Ziegler J F, Biersack J P and Littmark U 2008 *The Stopping and Ranges of Ions in Solids* vol 1 (New York: Pergamon) p 5

[16] Amano S, Inaoka Y, Hiraishi H, Miyamoto H and Mochizuki T 2010 *Rev. Sci. Instrum.* **81** 023104

[17] Komori H, Soumagne G, Hoshino H, Abe T, Suganuma T, Imai Y, Endo A and Toyoda K 2004 *Proc. SPIE* **5374** 839

[18] Ziegler J F, Biersack J P and Littmark U 1985 *The Stopping and Range of Ions in Matter* (2000 code) www.srim.org

[19] Henke B L, Gullikson E M and Davis J C 1993 X-ray interactions: photoabsorption, scattering, transmission, and reflection at $E = 50$–30000 eV, $Z = 1$–92 *At. Data Nucl. Data Tables* **54** 181